Baroclinic transport in the Gulf of Alaska Part II. A fresh water driven coastal current

by Thomas C. Royer[1]

ABSTRACT

A coastal geostrophic, baroclinic jet in the Gulf of Alaska is driven seasonally by fresh water discharge and winds. The narrow current (<20 km) has a mean transport of 0.24 × 10^6 m^3 s^{-1} (relative to 100 db) and velocities in excess of 66 cm s^{-1}. The jet reaches a maximum in autumn, coincident with maximum fresh water discharge along the coast. The wind, whose maximum is in January-February, affects this current to a lesser degree than fresh water. The linear response of the baroclinic transport anomalies to wind and fresh water anomalies is used to support cause and effect relationships.

The fresh, coastal current extends from Southeast Alaska into the western Gulf of Alaska and is the consequence of the accumulation of runoff beginning along the British Columbia coast. The Alaska Coastal Current and the Alaska Current are generally distinct from each other for the region sampled, with one notable exception near Kayak Island. The Alaska Coastal Current could be an important source of fresh water for the North Pacific Ocean.

1. Introduction

Severe meteorological conditions over the Gulf of Alaska act as forcing mechanisms for coastal circulation as well as producing conditions unfavorable to oceanographic sampling. The annual cycles of wind stress, air temperature and precipitation are extreme in the gulf, especially at the coast. Though hydrographic observations on the shelf of the northern Gulf of Alaska began as early as 1929 (Thompson *et al.*, 1936), the first seasonal data were not available until after 1970 (Royer, 1975). That seasonal study emphasized the influence of winds on the deep hydrographic structure over the shelf and was limited to less than two years of observations.

In order to describe the shelf circulation of the northern Gulf of Alaska, section lines were established across the shelf and adjacent waters in 1974 (Fig. 1). Salinity or conductivity-temperature-depth (STD/CTD) measurements were made at stations typically ten nautical miles apart. Seasonal coverage was attempted but not always achieved (Table 1). Sampling was carried out to within 10 m of the

1. Institute of Marine Science, University of Alaska, Fairbanks, Alaska, 99701, U.S.A.

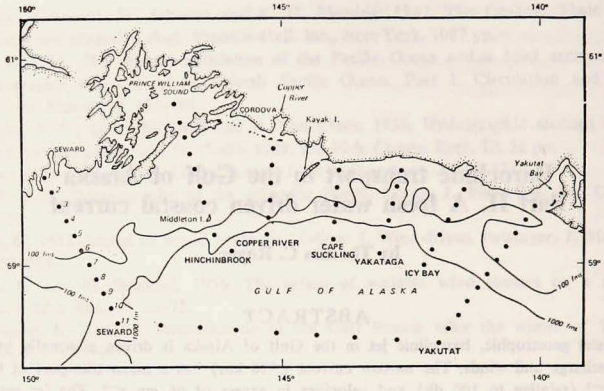

Figure 1. Northern Gulf of Alaska with hydrographic section names and station positions.

bottom or 1500 m whichever was less. Field calibrations were accomplished using reversing thermometers for temperature and water samples for comparison with standard sea water. Calibrations were done at depths where vertical gradients were minimal.

Some short term experiments (Hayes and Schumacher, 1976; Hayes, 1979) were part of the overall program. Those experiments indicate that wind stress causes a barotropic set-up over the shelf and bottom pressure gradient is uniform alongshore but diminishes offshore across the shelf. Flow perturbations near the shelf break do not propagate onto the shelf; thus shelf and deep ocean circulation are separate and distinct.

The relationship between coastal sea level and dynamic height in the northern Gulf of Alaska has been examined using a subset of the observations reported here (Royer, 1979). The seasonal cycle of dynamic height was found to be controlled by fresh water discharge in the upper 100 m and by wind stress in the lower layers (100 m-250 m). Observed seasonal variations in sea level are primarily a result of dynamic height fluctuations. While these results imply a seasonal variation in the baroclinic circulation, the dynamic heights from a single station cannot verify such a conclusion.

2. Hydrographic data and curve fitting technique

As an extension of that previous dynamic height study the hydrographic section data across the shelf are used to determine seasonal baroclinic transports and their anomalies. A total of 68 hydrographic transects from Yakutat to Seward (Fig. 1) have been occupied between 1974 and 1979 (Table 1). The 0/100 db

transport is selected to characterize the shelf circulation because few stations have maximum depths that were shallower than this depth. This depth is also typically the maximum depth of the seasonal mixed layer.

To test the existence of an annual transport cycle, the average 0/100 db baroclinic transports are determined for each month to construct an annual signal. This signal is fitted by a sinusoidal least-squares regression technique. This technique assumes a 12 month period and determines amplitude, and phase of the signal, while yielding the *F*-statistic to determine the quality of the fit. The symmetry of this fit assumes and forces the maximum and minimum to be separated by 6

Table 1. Distribution of hydrographic sections.

Section		J	F	M	A	M	J	J	A	S	O	N	D
Yakutat	1974							X					
(7)	1975						X			X		X	
	1976		X		X					X			
	1977												
Icy Bay	1974							X					
(8)	1975						X			X		X	
	1976		X		X					X		X	
	1977												
Yakataga	1974							X					
(7)	1975						X			X		X	
	1976		X		X					X			
	1977												
Cape Suckling	1974							X					
(7)	1975						X			X		X	
	1976		X		X					X			
	1977												
Copper River	1974							X			X		
(9)	1975						X			X		X	
	1976		X		X					X		X	
	1977												
Hinchinbrook	1974							X			X		
(8)	1975						X			X		X	
	1976		X		X					X			
	1977												
Seward	1974			X				X					
(22)	1975		X			X	X			X		X	
	1976		X	X	X			X		X		X	
	1977			X								X	
	1978					X			X	X			
	1979		X			X		X		X			

months. This procedure is the same as that in the accompanying paper (Royer, 1981).

3. Baroclinic transports

The mean baroclinic transports and their seasonal variations for the sections illustrated in Figure 1 are listed in Table 2. Transport comparisons between sections are not meaningful because the transects might not intersect the same proportion of the flow. For this reason, along-shore flow variability will not be considered here.

With the exception of the Seward transect, the mean transport over 0/100 db for these sections is 0.10-0.19 $\times$ 10^6 m^3 s^{-1} with annual amplitudes of 0.04-0.12 $\times$ 10^6 m^3 s^{-1} (Table 2). The maximum baroclinic flow is predicted for autumn (September-December), except for Cape Suckling and Icy Bay. The small F-value of the annual curve fit for Cape Suckling indicates this phasing is questionable. However, the Icy Bay fit with its significant confidence interval (>50%) agrees with the maximum found by Hayes and Schumacher (1976) and Hayes (1979). In those studies the currents over the Icy Bay transect are associated with wind stress. The peak transport for Icy Bay (Table 2) coincides with the maximum wind stress which occurs in February. The reason for the circulation to respond in this manner only at this location is not clear. For the Yakataga section, its high variability is in accord with the eddies found there by Hayes (1979) and Royer *et al.* (1979).

The frequent sampling of the Seward transect (Table 1) permits a more detailed analysis of the transport response to forcing mechanisms there. Twenty two transects comprise the data set with sub-samplings available for several of these transects (Table 1). The standard Seward transect consists of 11 stations with water depths ranging from 160 to 2400 m. The coast is very steep with depths greater than 200 m within 5 km of shore. Station 1 has a depth of 265 m. While the section is approximately orthogonal to the coast, it is not orthogonal to the bottom

Table 2. Mean transports ($\times 10^6$ m^3 s^{-1}) for 0/100 db $\pm$ amplitude of the seasonal variations (time of annual maximum) in the northern Gulf of Alaska.

Section			F	Confidence interval
Seward	1.19 $\pm$ 0.31	(Dec)	3.45	>50%
Hinchinbrook	0.10 $\pm$ 0.07	(Nov)	9.19	>90%
Copper River	0.19 $\pm$ 0.12	(Sept)	2.65	>50%
Cape Suckling	0.12 $\pm$ 0.05	(May)	1.46	–
Yakataga	0.13 $\pm$ 0.04	(Oct)	0.64	–
Icy Bay	0.12 $\pm$ 0.05	(Feb)	3.80	>50%
Yakutat	0.13 $\pm$ 0.08	(Nov)	1.26	–

contours at the shelf break. Consequently, this section better estimates nearshore flow than that of the Alaska Current, which is found immediately offshore of the shelf break (see Royer, 1981).

The annual harmonic fit of the 0/100 db transports for the entire Seward section (Stations 1-11) (Table 2) indicate a mean transport of 1.19×10^6 m^3 s^{-1} with an annual variation of $\pm .31 \times 10^6$ m^3 s^{-1}. For the entire section, the fit does not have high statistical significance due to the cross-shelf variability of the flow. This poor sinusoidal fit for the transport over the complete shelf is in contrast to the better fits for individual segments. Dividing the section into offshore (Stations 7-11) and coastal (Stations 1-7) segments on the basis of the 200 m isobath, the coastal flow has a significant (>99%) annual signal with a maximum in November (Table 3). The offshelf segment has an insignificant annual signal. The offshore and coastal transports (Fig. 2) display quite different characteristics. The offshore flow (Stations 7-11) has a much larger standard deviation ($.30 \times 10^3$ m^3 s^{-1}) than the coastal flow ($.17 \times 10^3$ m^3 s^{-1}) though their means are nearly identical (.60 versus $.61 \times 10^3$ m^3 s^{-1}). The coastal circulation generally increases from 1974 to 1976 and then declines (Fig. 2). No such pattern is evident for the offshore component.

Additional details of the annual transport fluctuations from individual station pair data (Table 3, Fig. 3) indicate that statistically the most significant annual

Table 3. Seasonal harmonic fits for baroclinic tranport of Seward section ($\times 10^6$ m^3 s^{-1}) for 0/100 db.

Station pair	Mean	Amplitude	Phase	F
1-7	.61	.23	Nov.	16.37[a]
7-11	.60	.08	Dec.	0.22
1-2	.12	.10	Jan.	19.38[a]
2-3	.24	.10	Oct.	13.33[b]
3-4	.13	.08	Dec.	4.24[d]
4-5	.07	.02	Nov.	0.61
5-6	.03	.02	Nov.	0.76
6-7	.02	.04	June	3.80[d]
7-8	.04	.06	Jan.	1.21
8-9	.14	.12	Dec.	5.09[d]
9-10	.12	.04	Sept.	0.19
10-11	.30	.09	May	1.08

For $F_{1,7}$

	F	P$\geqslant$
a	16.20	99%
b	8.07	95%
c	5.59	90%
d	3.59	80%
	1.57	50%

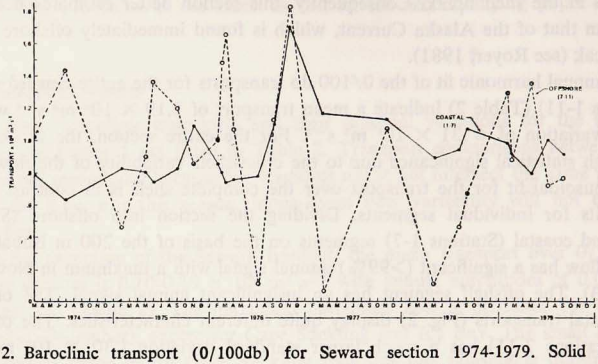

Figure 2. Baroclinic transport (0/100db) for Seward section 1974-1979. Solid line for coastal (Stations 1-7) and dashed line for offshore (Stations 7-11) transports.

signal is for the station pair at the coast (Stations 1-2). Progressing offshore, the mean transport doubles for Stations 2-3 and its annual amplitude remains constant. From Stations 2-3 to Stations 6-7 the mean flow decreases with the probability that an annual signal exists becoming insignificant ($P<50\%$ for Stations 4-6). The transport for Stations 6-7 is out of phase with the other transports over the shelf by about 180°. The phasing of the seasonal transport signal for Stations 8-9 appears coupled to the minimum at Stations 6-7 for the same time. Significant annual transport signals are not found for the outer two station pairs.

The small-scale temporal variations of nearshore transport can be determined from hydrographic data for 22-25 February, 2 March and 4-5 March 1976 (Table 4). Over this period the offshore (0/100 db) transport nearly doubles. The coastal (0/100 db) transport also decreases slightly in a linear fashion. The consistency of this shelf transport over this time period, suggests that; (1) the transport time-accelerations over the nearshore shelf are small and (2) the precision of the baroclinic transport computation is of the order of 0.05×10^6 m^3 s^{-1}. The 0/1500 db transport for the entire section has a significant increase throughout the period with changes occurring in excess of 2.2×10^6 m^3 s^{-1} over several days. This acceleration is caused by rapid changes in the offshelf transport, which are probably a result of the lateral displacement of the Alaska Current.

To investigate the spatial scale of the coastal current, a very closely sampled (3.7 km) transect between Stations 1 and 3 was taken on 11 September 1979. The flow is not revealed in the temperature distribution (Fig. 4a), but is detailed in the salinity distribution (Fig. 4b). The cross-shelf distribution of velocities (Fig. 4c) indicate the major axis of a coastal jet which is 5-10 km wide. The standard station spacing of 18.5 km for the Seward transect is therefore too

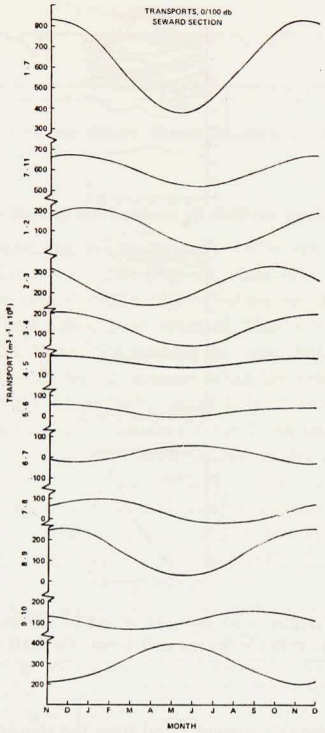

Figure 3. Annual baroclinic transport cycles from curve fitting procedure for segments and station pairs on Seward section, (0/100db).

coarse to resolve adequately the horizontal details of the velocity profile. All transport computations are valid, however, since they are independent of station spacing. The standard transect with 18.5 km spacing taken two days earlier produced dynamic height gradient that differed by one least count (0.001 dyn. m.) from the more finely sampled transect. Over the two-day period between these two transects, there are decreases of 0.007 and 0.006 dyn. m. (0/100 db) for Stations 1 and 2 respectively. These decreases are consistent with net dilution from fresh water discharge at that time of the year and add support to a hypothesis that will be developed later in this paper, that this is a fresh water driven coastal jet.

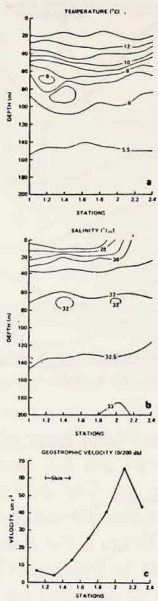

Figure 4. Detailed cross section of a) temperature and b) salinity with a geostrophic speed profile c), for September 1979 for Seward section near the coast (See Figure 1 for positions of Stations 1 and 2).

The maximum geostrophic current speed from the standard section is 37 cm s^{-1} whereas the finer section has a maximum speed of 66 cm s^{-1} (Fig. 4). The standard section will underestimate current speeds. The position of the coastal current axis beyond 20 km from the coast might not be characteristic of the current's position elsewhere along this coast since the coast is irregular, especially near the Seward transect.

Table 4. Seward section transports, February-March 1976, ($\times 10^6$ m^3 s^{-1}).

	Coastal 0/100 db	Offshore 0/100 db	Coastal 0/200 db	Total 0/1500 db
22-25 Feb.	.55	.70	.70	2.30
2 March	.50	1.18	.64	4.92
4- 5 March	.44	1.35	.56	7.14

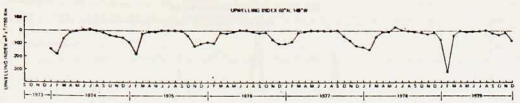

Figure 5. Upwelling index (onshore-offshore Ekman transport) for 60N. 149W. from 1973-1979.

4. Wind and fresh water forcing mechanisms of shelf circulation

The monthly mean upwelling indices for 60N, 149W are used as a measure of the onshore-offshore Ekman transport (Fig. 5), since direct wind measurements are not available for the coastal region. These indices are determined from large scale grids of 6 hr sea-level atmospheric pressure. Their computation is discussed elsewhere (Bakun, 1973). Errors are possible in these data; in winter when the magnitudes are overestimated and in summer when the predicted westerly winds that cause upwelling might not actually occur (Livingstone and Royer, 1980). These problems do not invalidate the data from being used to represent wind forcing since seasonal transitions are correct; intense winter downwelling and very small wind magnitudes in summer. The winter downwelling, whose time of maximum ranges from November to February, flushes the shelf with relative low salinity water through a coastal convergence (Royer, 1975). The absence of downwelling in summer allows warm, saline water to intrude onto the shelf in the near-bottom layers.

As mentioned earlier, fresh water discharge along the coast is a potential driving mechanism for the coastal circulation. The discharge is quite uniform along this coast. There are few major rivers, but instead numerous small streams drain the mountainous coastline. Thus, the fresh water discharge is dependent on the local precipitation and rate of snow melt, the latter depending on air temperatures and insolation. To estimate the fresh water discharge, a model is used similar to that employed in Royer (1979), where further details are available. The slight difference in this new model is that interannual storage or release of fresh water is allowed if anomalous temperatures occur. A 600 km alongshore and 150 km wide coastal drainage is employed with monthly mean precipitation and temperatures for the Alaska southcoast division being used as input. The Alaska southcoast division, as defined by the National Weather Service, extends from Yakutat to Seward and inland to include Prince William Sound. Water storage as snow is allowed when temperatures are less than 0°C. The rate of change of meltwater is assumed to occur in a linear fashion and the only gauged discharges, the Copper River (Fig. 1), are added directly. This river's watershed area is primarily in interior Alaska and therefore does not reflect coastal conditions.

The fresh water discharge from the model has its maximum in early fall,

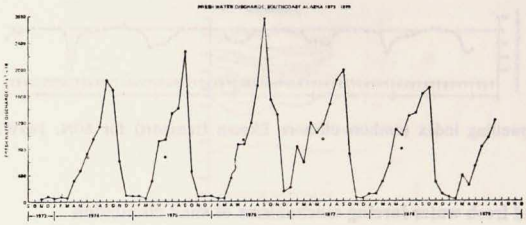

Figure 6. Fresh water discharge, southcoast Alaska based on 150 km with hydrology model. 1973-1979. (Open circles are the mean annual discharge rate.)

usually September, with small flows during winter (December-March) (Fig. 6). Spring break-up often produces a submaximum (usually in May) followed by a brief decline and then a rapid increase in discharge into the summer months. The maximum and mean annual (open circles, Fig. 6) discharges increase from 1973 to 1976. While the greatest monthly discharge 27.6 $\times$ 10^3 m^3 s^{-1} was in September 1976, the year with the greatest annual mean discharge (9.24 $\times$ 10^3 m^3 s^{-1}) was 1977.

The variation across the shelf in the seasonal transport signals (Fig. 3) can be attributed to the phasing of the forcing mechanisms. The January maximum flow at the coast over the Seward Line could be due to the downwelling maximum which occurs at the time. For those station pairs further offshore, the peak shifts to early in fall as the result of fresh water discharge which is a maximum at that time.

The significant annual signals for Stations 6-7 and 8-9 are a consequence of the upstream bifurcation of the coastal jet by Kayak and Middleton Islands (Fig. 1). The jet which is separated from the coast upstream, appears as a fresh water filament approximately between Stations 7 and 8. The slope of the horizontal pressure gradient will change sign across this filament. Thus, the feature will cause eastward acceleration on its shoreward side and westward acceleration on its offshore side. Low salinity surface water associated with this flow has been reported by Favorite *et al.* (1976) and Ingraham (1979). Stratification from this low salinity stream allows uniform incident radiation to develop a horizontal temperature gradient at the surface through differences in vertical mixing. The lens is detectable in the sea surface temperature and has been reported by Royer and Muench (1977).

For Stations 9-10, the very low confidence level of the annual signal could be the result of contamination of the annual signal by eddies propagating along the shelf break, which were reported in Royer and Muench (1977), Hayes (1979) and Niebauer *et al.* (1981). These eddies are a mechanism of momentum exchange be-

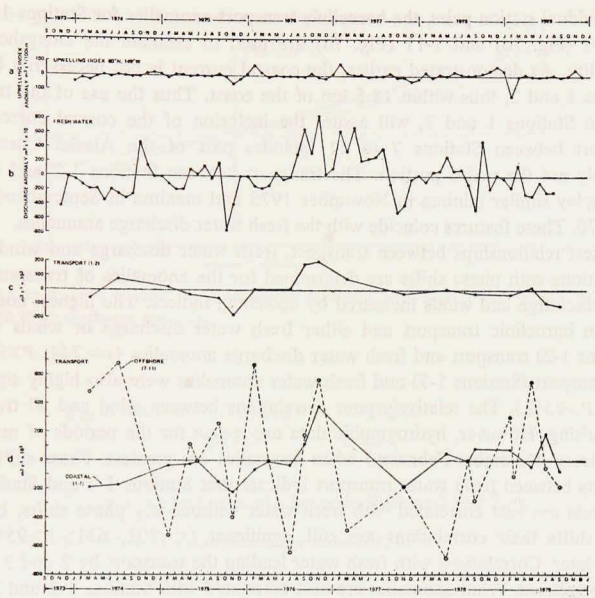

Figure 7. Anomalies of a) upwelling index, b) fresh water discharge, c) baroclinic transport between Stations 1 and 2 of the Seward section, and d) baroclinic transport for coastal (solid) and offshore (dashed) segments of Seward section from 1973 to 1979.

tween the Alaska Current and the shelf waters. The high transport for the Alaska Current (Stations 10-11) is not associated with a strong annual signal since eddies or meanders of the Alaska Current could play an important role here, too.

5. Wind, fresh water and transport anomaly analysis

The relatively large seasonal amplitudes of wind and fresh water transport interfere with cross-correlation analysis of these signals. For example, all annual signals will be well correlated at some particular phase shift, even if there is no cause-effect relationship. To avoid such erroneous results, the monthly means are subtracted from the upwelling index, fresh water discharge and baroclinic transport data, leaving anomalies from the annual signal. The upwelling index anomaly (Fig. 7a) was positive in late winter 1976 and 1977 with a large negative anomaly in February 1979. The fresh water discharge anomaly generally increases from 1973 through 1976 with a decline into 1979 (Fig. 7b). Instead of addressing

all individual station pairs, the baroclinic transport anomalies for Stations 1-2 (Fig. 7c), 1-7 (Fig. 7d) and 7-11 (Fig. 7d) are used to estimate the alongshore flow variability. As demonstrated earlier, the coastal current is not necessarily between Stations 1 and 2, thus within 18.5 km of the coast. Thus the use of the transport between Stations 1 and 7, will assure the inclusion of the coastal current. The transport between Stations 7 to 11 includes part of the Alaska Current but probably not the major portion. The transport between Stations 1-2 and Stations 1-7 display similar minima in November 1975 and maxima in September-November 1976. These features coincide with the fresh water discharge anomalies.

To test relationships between transport, fresh water discharge and wind, cross-correlations with phase shifts are determined for the anomalies of transport, fresh water discharge and winds measured by upwelling indices. The highest correlation between baroclinic transport and either fresh water discharge or winds was for (Stations 1-2) transport and fresh water discharge anomalies (r=.744; P>99.9%). The transport (Stations 1-7) and fresh water anomalies were also highly significant (.588; P>95%). The relatively poor correlations between wind and all transports is surprising. However, hydrographic data are sparse for the periods of maximum wind stress (December-February) when anomalies are greatest. Phase-shifted correlations between fresh water transport indicate that Stations 1-2 and Stations 1-7 transports are best correlated with fresh water without any phase shifts, but with phase shifts their correlations are still significant (r=.701, 631; P>95%) one month later. Correlations with fresh water leading the transport by 2 and 3 months are insignificant. Wind anomalies are best correlated with Stations 1-2 and Stations 1-7 transport anomalies when the winds lead the transport by one month. Wind anomalies with this lead are better correlated with Stations 1-7 transport (.472) than Stations 1-2 transport (.338). In summary, variations in the coastal current can be attributed primarily to fresh water discharges and secondarily to prior local winds.

The linear response of the alongshore baroclinic transport to the fresh water discharge (Fig. 8) is greater for Stations 1-7 transport than Stations 1-2 transport, which once again implies that the coastal current response to fresh water is not confined to within 18.5 km of the coast. This agrees with the results of the detailed transect. The linear fits for the baroclinic responses to fresh water discharge anomalies have F statistics of 10.61 (P>99%) for Stations 1-7 transport and 19.82 (P>99.9%) for Stations 1-2 transport.

The combined effects of fresh water and winds on the transport are tested through a multiple linear regression analysis. The linear responses with the smallest residual sums of squares are

$$T_{1\text{-}7} = -6.7 + \underset{(7.17)}{.02336 f} + \underset{(2.15)}{2.122 W(+1)}$$

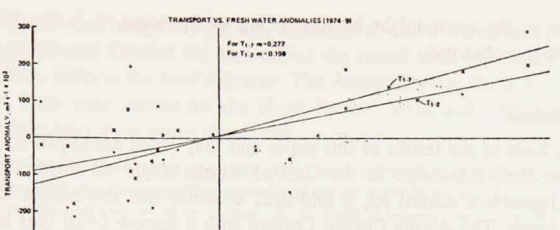

Figure 8. Linear, least squares fit of baroclinic transport anomalies from Seward section to the fresh water discharge anomaly.

and

$$T_{1\text{-}2} = 10.1 + \underset{(18.13)}{0.01845\, f} + \underset{(.85)}{.3400\, W},$$

where

$T_{1\text{-}7}$ = transport anomaly, between Stations 1 and 7, $m^3\ s^{-1} \times 10^{-3}$

f = fresh water discharge anomaly, $m^3\ s^{-1}$

W = upwelling index anomaly, $m^3\ s^{-1}/100$ m of coastline.

The "best fit" to $T_{1\text{-}7}$ is accomplished with fresh water in phase but with winds leading the transport by one month. For $T_{1\text{-}2}$, the fresh water and winds are in phase with the transport. F-statistics for the regression are in parentheses beneath the individual coefficients. The transport has a better fit to fresh water very near the coast, whereas winds become more significant at greater distances from the coast. The validity of this analysis is related to the independence of the "independent variables"; fresh water and wind. They are poorly correlated when in phase (r=.140) but are well correlated when the wind leads fresh water by one month (r=.542) and hence are not necessarily independent. Their dependence could be from storm systems increasing the winds and releasing precipitation which in turn enters the ocean in a delayed manner.

The delayed response to the wind at greater distances from the coast can be observed in the transport anomaly phase shift for $T_{1\text{-}2}$ versus $T_{1\text{-}7}$. This shift is possibly a consequence of Ekman dynamics. The internal Rossby radius of deformation for the coastal current here ranges from 5 to 20 km, depending on stratification. Therefore, the direct wind response is expected to be confined to the station pairs adjacent to the coast. However, it is within this coastal band that the major fresh water influx occurs and can override the wind effect. While the

circulation at the coast might be responding to the wind, it is the fresh water response that is observed.

6. Conclusions

On the basis of the results of this paper and that which accompanies it (Royer, 1981), the shelf circulation in the Gulf of Alaska might be divided into three different regimes; a coastal jet, a mid-shelf doldrum and the Alaska Current at the shelf break. The Alaska Coastal Current with a narrow (~10 km) high speed core (>60 cm s^{-1}) and relatively high peak baroclinic transports (>1 × 10^6 m^3 s^{-1} for 0/100 db) is driven by coastal fresh water discharge and local winds. Because fresh water is accumulated within this band, the flow could be influenced by distant precipitation and runoff from the British Columbia and Southeast Alaska coasts. Satellite-tracked drifters have been transported by this coastal jet beginning at about 140W and terminating in Prince William Sound (Royer *et al.*, 1979). Kirwan *et al.* (1978) also have evidence from drifters of a coastal current near Sitka (55N, 134W), likely to be part of this same Alaska Coastal Current. The Kenai Current reported by Schumacher and Reed (1980) represents a component of the Alaska Coastal Current. The Alaska Coastal Current transport is a maximum in fall coincident with maximum fresh water discharge rates and a minumum in spring prior to spring break-up.

The potential for the fresh water forcing of ocean circulation has been recognized for the Southern Ocean. Johnson (1979) discusses the effect of precipitation on zonal flow, and indicates that the subsequent redistribution of mass generates a circulation that is similar to that resulting from wind stress alone. However, the forcing mechanism of fresh water differs from that of wind stress since the fresh water is cumulative and drives the flow unidirectionally along a boundary. Coriolis effects keep this flow adjacent to the coast when the coast is to the right of the flow. The fresh water forcing is possible here only because of the very large discharge rate and the nonlinear nature of the equation of state of sea water. This nonlinearity increases the effect of salinity changes on the density at low temperatures. The fresh water enters the marine system here as numerous small rivers and streams with an annual discharge per km of coastline being .41 km^3 for a 150 km wide watershed. This is in contrast with .39 km^3 for the northern Gulf of Mexico where the water enters via large rivers such as the Mississippi (Meade and Emery, 1971).

The concept that fresh water is important to circulation in the Gulf of Alaska is not a new one. Tully and Barber (1960) treated the region as an estuary, but did not have the data to investigate the temporal and spatial variability. As an extension of their discussion, however, the Alaska Coastal Current and the Alaska Current are emphasized here as distinct in the northern Gulf of Alaska, but large

scale water and heat budgets require an exchange of salt and heat across the shelf. The Alaska Coastal Current will also advect the runoff from one area to another, causing phase shifts in the flow response. The Alaska Coastal Current could be an important fresh water source for the North Pacific Ocean and hence play an important role in large scale ocean circulation.

Acknowledgments. Many ships and their crews have assisted in the gathering of the data discussed here, but special recognition must be given to recently retired R. V. *Acona* which was used for the majority of these cruises. R. O. Reid developed the curve fitting routine. J. Colonell, D. Nebert and J. Niebauer provided input on this manuscript. This work was supported by the BLM/NOAA OCSEA Program and by NORPAX, an NSF, IDOE Program. Institute of Marine Science Contribution No. 435.

REFERENCES

Bakun, A. 1973. Coastal upwelling indices, west coast of North America, 1946-71. U.S. Dep. Commer. Natl. Oceanic Atmos. Admin. Tech. Rept. NMFS SSRF-671. 103 pp.

Favorite, F., A. J. Dodimead and K. Nasu. 1976. Oceanography of the sub-arctic Pacific region, 1960-72. Int. N. Pac. Fish. Comm. Bull., *33*, 187 pp.

Hayes, S. P. 1979. Variability of current and bottom pressure across the continental shelf in the northeast Gulf of Alaska. J Phys. Oceanogr., *9*, 88–103.

Hayes, S. P. and J. D. Schumacher. 1976. Description of wind, current and bottom pressure variations on the continental shelf in the Northeast Gulf of Alaska from February to May 1975. J. Geophys. Res., *81*, 6411–6419.

Ingraham, W. J. Jr. 1979. The anomalous surface salinity minima area across the northern Gulf of Alaska and its relation to fisheries. Mar. Fish. Rev., *41*, 8–19.

Johnson, J. A. 1979. A wind-driven zonal channel with stratification and bottom topography. Dynamics of Ocean. and Atmos., *4*, 1–13.

Kirwan, A. D. Jr., G. J. McNally, E. Reyna and W. J. Merrell Jr. 1978. The near surface circulation of the eastern North Pacific. J. Phys. Oceanogr., *8*, 937–945.

Livingstone, D. and T. C. Royer, 1980. Observed surface winds at Middleton Island, Gulf of Alaska and their influence on ocean circulation. J. Phys. Oceanogr., *10*, 753–764.

Meade, R. H. and K. O. Emery. 1971. Sea level as affected by river runoff, eastern United States. Science, *173*, 425–428.

Niebauer, H. J., T. C. Royer and M. J. Roberts. 1981. Shelf break circulation in the northern Gulf of Alaska. J. Geophys. Res., *86*, (in press).

Royer, T. C. 1975. Seasonal variations of waters in the northern Gulf of Alaska. Deep Sea Res., *22*, 403–416.

—— 1979. On the effect of precipitation and runoff on coastal circulation in the Gulf of Alaska. J. Phys. Oceanogr., *9*, 555–563.

—— 1981. Baroclinic transport in the Gulf of Alaska Part I. Seasonal variations of the Alaska Current. J. Mar. Res., *39*, 239–250.

Royer, T. C. and R. D. Muench. 1977. On the ocean temperature distribution in the Gulf of Alaska, 1974-1975. J. Phys. Oceanogr., *7*, 92–99.

Royer, T. C., D. V. Hansen and D. J. Pashinski. 1979. Coastal flow in the northern Gulf of Alaska as observed by dynamics topography and satellite-tracked drogued drift buoys. J. Phys. Oceanogr., *9*, 785–801.

Schumacher, J. D. and R. K. Reed. 1980. Coastal flow in the Northwest Gulf of Alaska: The Kenai Current. J. Geophys. Res., *85*, 6680–6688.

Thompson, T. G., G. F. McEwen and R. VanCleve. 1936. Hydrographic sections and calculated currents in the Gulf of Alaska, 1929. Int. Fish. Comm. Rept. 10. 32 pp.

Tully, J. P. and F. G. Barber. 1960. An estuarine analogy in the sub-arctic Pacific Ocean. J. Fish. Res. Bd. Can., *17*, 91–112.

Received: *15 July, 1980;* revised: *20 November, 1980.*